JNTM JOURNAL of NEW TECHNOLOGY and MATERIALS

Journal of New Technology and Materials

Vol. 14, No. 2 (2024), 47–57

RESEARCH ARTICLE

Carbon-State-Gated Interface Normalisation of Exsolved Nickel–Lanthana Catalysts for Low-Temperature CO_2 Methanation

Umer Shehzad[1,*], Fatima Zehra[1] and Anjum Hussain[1]

[1]Department of Chemistry, University of Education, Lahore campus, 54000, Pakistan

*Correspondence: umershehzad12@gmail.com

Received date: August 21, 2023; Accepted date: September 02, 2024

Abstract

Nickel–lanthana-based catalysts synthesised from $LaNiO_3$ perovskite precursors are interesting materials for low-temperature CO_2 methanation due to their unique combination of active sites for hydrogen activation and oxygenated carbon compounds adsorption. The key point is to understand which of those states offers the optimal interface for catalytic methanation based on the interconnection between catalyst activity, crystal size, apparent activation energy, phases, and carbon surface chemistry. This study reveals the answer to the question above using a carbon-state-gated interface normalisation. It integrates thermal activation gain with respect to the impregnated Ni/La_2O_3 catalyst, light-off gain ratio, size-adjusted activity gain corrected by the apparent activation energy value, and oxygenates gate factor based on La 3d spliting and surface carbonate-to-lanthanum ratio. As a result of calculations, $LaNiO_3$-600 is found to be the preferred interface state since it yields 50% CO2 conversion at 285 °C that is 96 °C lower temperature compared to the impregnated Ni/La_2O_3 catalyst, 25.2 % light-off gain, apparent activation energy 87 kJ mol^{-1}, and the highest size-normalised activity gain 12.83 °C nm^{-1}. It is concluded that the performance advantage is not associated with nickel crystallite size itself but results from coupling between accessible metallic nickel and lanthanum surface available for oxygenates adsorption rather than being blocked by carbonate cover.

Keywords: CO_2 methanation, $LaNiO_3$, exsolved nickel, lanthanum oxycarbonate, carbon-state gate, Sabatier reaction, materials descriptor, nickel–lanthana interface

1 Introduction

Carbon dioxide conversion into methane through catalysis is both a reaction engineering and materials problem. Overall, the process is defined by the Sabatier reaction,

$$CO_2 + 4\,H_2 \longrightarrow CH_4 + 2\,H_2O. \tag{1}$$

However, this deceptively simple equation means that four molecules of hydrogen must interact with a molecule of carbon dioxide and produce methane and two molecules of water with high selectivity. For a catalyst, this implies that hydrogen splitting, CO_2 adsorption, weakening of the *C-O* bond, hydrogenation of the intermediates, and water desorption should happen in coordination in an interfacial region. This makes catalysis by nickel not merely a matter of its presence as a metal and a function of its interaction with a basic oxide support. Instead, the key is whether a combination of phases forms an interface where hydrogen and carbon-oxygen complexes can move through the same chemical space [1–3].

A crucial role of nickel in methane formation has been recognised because this metal yields high selectivity of product formation without noble metal costs. The challenge is that nickel can be neither a stable metal in the reaction nor an efficient active phase. Particle movement, agglomeration, oxidation-reduction cycling, carbon deposition, and adsorption of strong intermediates can lead to reduced surface area. Moreover, nickel particle sizes are critical for determining the

distribution of steps, edges, and terraces necessary for the hydrogenation sequence. While small particles will ensure dispersion of the phase, the interfacial zone where carbon-oxygen species are delivered to nickel is important. Similarly, large particles will yield high efficiency if the interface with the oxide ensures delivery of activated carbon–oxygen species to the hydrogenation centres. In other words, the relevant question concerns not merely the amount of the metal but the properties of the metal–oxide interface formed during synthesis.

Lanthana-based catalysts offer good opportunities to address this problem. The La_2O_3 phase can adsorb carbon dioxide, undergo hydroxylation in humid environments, and transform into carbonate and oxycarbonate. This property can either be beneficial for catalysis or detrimental. A labile hydroxide and oxycarbonate layer may help activate CO_2 species and deliver them to nickel for hydrogenation. At the same time, carbonates may prevent effective turnover of carbon–hydrogen complexes by occupying active positions in the interface. Indeed, the literature on nickel-lanthana catalysts demonstrates a clear controversy: while carbonates can help to activate CO_2, excessive carbonate accumulation in some materials can inhibit turnover of carbon and hydrogen complexes [4–6].

Perovskite-derived catalysts represent a means of regulating the interface better than impregnation processes. In $LaNiO_3$, nickel is incorporated in the oxide lattice. By reducing $LaNiO_3$ in hydrogen, it can form nanoparticles in direct contact with or strongly attached to the lanthanum-rich oxide substrate. The presence of exsolved particles results in higher resistance to sintering due to the stronger connection of nickel with the parent oxide than the one formed during impregnation. However, this example illustrates why exsolution cannot be considered the main factor in determining catalyst performance. Depending on the hydrogen activation temperature, the degree of perovskite decomposition, metallic nickel crystallite size, and extent of surface hydroxylation, carbonate and oxycarbonate phases can form on the surface. As a result, the active catalyst state represents a product of thermally driven interface evolution.

Current knowledge about exsolved $LaNiO_3$-based catalysts allows proposing that lanthanum surface modification can be crucial besides particle formation. Near-ambient pressure spectroscopic studies show that surface La-hydroxides may predominate over hexagonal La-carbonates in exsolved nickel-lanthana catalysts, while La-carbonates accumulate on the surface of impregnated samples [7]. This finding matters for the present work because it changes the perspective of the analysis away from the traditional approach focused on particle sizes. Instead, comparing exsolved and impregnated nickel-lanthana catalysts requires taking into account the carbon state of lanthanum, apparent activation energy, light-off temperature, and nickel crystallites.

The aim of this study is therefore to identify which of the two interfaces (exsolved vs. impregnated) is most effective for low-temperature methanation by considering the catalyst state. The latter refers to light-off temperature, apparent activation energy, crystallite size, lanthanum surface modifications, and carbonate chemistry. For achieving this goal, a materials-ranking protocol based on carbon state gated interface normalization has been developed. The proposed method estimates the difference in thermal activation gain from the impregnated Ni/La_2O_3 catalyst to the material being studied. This value is then converted to the percentage increase of light-off point. Then, the normalized light-off improvement is calculated from the ratio between the gain and nickel crystallite size and apparent activation energy. Finally, the oxygenate gate of each interface has been determined from the surface markers of lanthanum. The novelty of the ranking protocol does not concern the replacement of turnover frequency studies or kinetic analysis. Instead, it offers a transparent way of comparing similar catalysts based on the available information.

The novelty is thus in treating nickel-lanthana interfaces in perovskite derivatives as adaptive surfaces where the performance depends on simultaneous development of a metallic catalyst and lanthanum carbonate chemistry. The most effective material should exhibit accessible nickel nanoparticles, low apparent activation energy, intact interface, and open hydroxide/oxycarbonate-compatible lanthanum surface state. This position clearly fits new technology materials research because catalysis by nickel is understood as an artificial creation of an interface based on phase transformation and nanometal formation.

2 Protocol of carbon-state-gated calculation

2.1 Interface normalisation by carbon-state gate

The present calculation takes the starting point of assuming that the methanation on nickel–lanthana systems demands two simultaneous functions. On the one hand, the metallic nickel activates H_2 and hydrogenation sites. On the other hand, the lanthanum-based oxide provides oxygen-containing bases necessary to take up CO_2 and transform it into carbon–oxygen intermediate species. The functionality becomes productive only if the interface between the two is kept chemically accessible. Indeed, although a highly carbonate-loaded lanthanum surface demonstrates a high affinity to CO_2, high affinity is not synonymous with high turnover if the adsorbed intermediate cannot be readily hydrogenated. Similarly, a surface that is open to hydroxide or oxycarbonate species can still function as an oxygenate carrier if it remains in close proximity to metallic nickel.

The first descriptor of interest is the thermal activation gain, relative to the impregnated Ni/La_2O_3 comparator:

$$\Delta T_{50,i} = T_{50,\mathrm{ref}} - T_{50,i}, \tag{2}$$

where $T_{50,i}$ denotes the temperature needed to achieve 50 % CO_2 conversion over the i^{th} catalyst in the series, and $T_{50,\text{ref}}$ refers to the respective value for impregnated Ni/La_2O_3. The equation represents the temperature gap in degrees Celsius, rather than the difference in conversion at a fixed temperature. The positive value implies that the catalyst reaches the same conversion target with lower energy expenditure. The formulation is convenient in cases where one wishes to compare materials derived from the same chemical compound.

The light-off improvement can be defined as follows:

$$L_i = \frac{\Delta T_{50,i}}{T_{50,\text{ref}}} \times 100. \tag{3}$$

Eq. (3) describes the temperature reduction as a proportion of the reference light-off demand. Although the value represents a percentage improvement, it should not be regarded as a thermodynamic efficiency parameter. Instead, it constitutes a comparative measure, designed not to misinterpret the extent of low-temperature gain irrespective of the reference value. In the current example, L_i makes it possible to evaluate the three hydrogenated forms of $LaNiO_3$ alongside the same impregnated analogue in terms of their original T_{50} values.

The second descriptor is the size-normalised activity gain,

$$N_i = \frac{\Delta T_{50,i}}{D_{\text{Ni},i}} \left(\frac{E_{\text{app,ref}}}{E_{\text{app},i}} \right), \tag{4}$$

where $D_{\text{Ni},i}$ corresponds to the nickel crystallite size, and $E_{\text{app},i}$ represents the apparent activation energy. Eq. (4) purposely reduces the score of the catalyst if the advantage in light-off is attained only by shrinking the size of its nickel crystallites. Only if the light-off and apparent kinetic barrier ratios are in favor of the catalyst will the latter gain the additional credit. Therefore, N_i is an indicative comparison of materials rather than an intrinsic property. The descriptor has validity only in comparative analyses of similar catalysts.

The third descriptor is the lanthanum oxygenate gate, G_i, which has to be estimated based on the La 3d band splitting and the stoichiometric ratio of surface carbonate ions to total lanthanum atoms:

$$G_i = \begin{cases} \text{open}, & \Delta_{\text{La 3d}} \approx 3.6\,\text{eV},\ {CO_3}^{2-}/\text{La} \ll 1, \\ \text{blocked}, & \Delta_{\text{La 3d}} \approx 3.4\,\text{eV},\ {CO_3}^{2-}/\text{La} \approx 1.5, \\ \text{undetermined}, & \text{insufficient surface-state information.} \end{cases} \tag{5}$$

In Eq. (5), a distinction is made between the physically carbonated surface and the one that is chemically accessible as an oxygenate reservoir. An open gate indicates that the lanthanum-based surface is capable of hydroxide and oxycarbonate exchanges, whereas a closed gate means that a high concentration of carbonate-containing species blocks access to the metal–oxide junction. The criterion is based on knowledge about the stability of lanthanum oxycarbonates and hydrated lanthanum carbonates; however, it is also confirmed by recent methanation studies demonstrating that the role of carbonate in methanation is contingent on the nature of interactions, stoichiometry, and proximity to nickel [7–9].

2.2 Sequence of calculations

The following calculation scheme comprises three consecutive steps. First, a rank is determined from the T_{50}, E_{app}, and ΔT_{50} data. Next, the light-off gain is divided by the nickel crystallite size and multiplied by the activation-energy ratio to calculate N_i. Finally, the gate status is assigned from the available surface-state information. The ultimate judgment is formed only by comparing the rank with the carbon-state gate. If the former is high but the gate is blocked, the catalyst cannot be considered ideal because its high response potential would not have a chemically open pathway for repeated hydrogenations of the intermediate. A catalyst with modest nickel domain size, reduced apparent kinetic barrier, high N_i, and an open gate is deemed favourable.

3 Descriptor values and catalyst inputs

Values included in the catalyst set are necessary to compare catalytic efficiency, structural features, and surface-state properties of four states: $LaNiO_3$-400, $LaNiO_3$-500, $LaNiO_3$-600, and impregnated Ni/La_2O_3. Notations $LaNiO_3$-x refer to a $LaNiO_3$-based material activated with hydrogen in 400 °C, 500 °C, or 600 °C temperatures. Standard of comparison in the problem is a Ni/La_2O_3-based material activated in hydrogen at 600 °C. Values available for analysis are sufficient because they encompass light-off temperature, apparent activation energy, nickel crystallite size, lanthanum oxide domain size, lanthanum phase identity, and surface oxygenate markers. The main advantage of the comparison is that all catalyst states involve nickel and lanthanum. Therefore, ranking of these states depends on differences between their structural architecture and carbon-state accessibility.

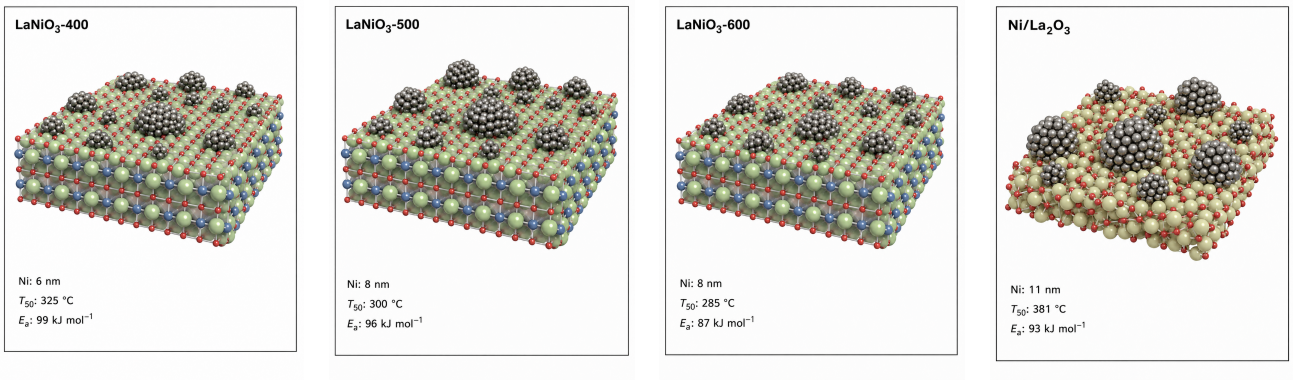

(a) $LaNiO_3$-400. **(b)** $LaNiO_3$-500. **(c)** $LaNiO_3$-600. **(d)** Ni/La_2O_3.

Figure 1. Comparison of catalyst states used for carbon-state-gated analysis. The four panels visualise activated perovskite-based materials and a comparative impregnated material so that their nickel crystallite size, T_{50}, and apparent activation energy can be compared along with descriptor table.

Figure 1 provides a starting point for the analysis. Perovskite-based states are not representative of individual catalysts but progressive steps in thermal activation of the same $LaNiO_3$ material. Impregnated Ni/La_2O_3 material serves as standard in which nickel is deposited onto a lanthanum oxide support rather than generated from perovskite. Comparison in Figure 1 separates two factors that may otherwise be confused: size of the nickel crystallites and chemical method by which the lanthanum-nickel interface is created. The latter becomes especially relevant in further analysis because the best performing material is not the one with the smallest crystallites, but the one with most favourable combined kinetic state and oxygenate state.

Table 1. Performance parameters for carbon-state-gated interface normalisation.

Catalyst	T_{50} (°C)	E_{app} (kJ mol^{-1})
$LaNiO_3$-400	325	99
$LaNiO_3$-500	300	96
$LaNiO_3$-600	285	87
Ni/La_2O_3	381	93

According to Table 1, perovskite-based catalysts have significantly lower light-off temperature compared to the impregnated material. While the $LaNiO_3$-600 catalyst achieves 50 percent conversion of methanol at 285 °C, the comparator requires 381 °C to achieve the same degree of conversion. 96 °C difference is too great to be attributed to experimental variation or a slight shift in temperature at which conversions start. On the contrary, activation of a perovskite catalyst in hydrogen under 600 °C creates a catalyst state with a distinctly different kinetic profile. In addition to the above consideration, a comparison of apparent activation energy in Table 1 reveals that catalysts $LaNiO_3$-400 and $LaNiO_3$-500 lower T_{50} but still exhibit higher apparent activation barriers compared to the comparator, while $LaNiO_3$-600 exhibits the lowest T_{50} and E_{app}. Thus, $LaNiO_3$-600 has a superior combination of the two parameters.

Table 2. Structural descriptors useful for understanding lanthanum-nickel interaction and evolution of lanthanum phases.

Sample	S_{BET} (m^2 g^{-1})	D_{Ni} (nm)	D_{LaOx} (nm)	Main La-containing crystalline phase
$LaNiO_3$	3	–	–	$LaNiO_3$
$LaNiO_3$-400	2	6	12.9	$LaNiO_3$, h-La_2O_3
$LaNiO_3$-500	<1	8	14.5	h-La_2O_3
$LaNiO_3$-600	<1	8	17.5	h-La_2O_3
spent $LaNiO_3$	–	–	17.3	h-$La_2O_2CO_3$, h-La_2O_3
Ni/La_2O_3	<1	11	18.9	h-La_2O_3
spent Ni/La_2O_3	–	11	19.5	h-La_2O_3

Table 2 prevents the performance ranking from being reduced to a single surface-area argument. The BET areas are all very low, so the improved methanation response of the perovskite-derived catalysts cannot be credited to a large area difference. The important changes are instead the nickel-domain size and lanthanum phase evolution. $LaNiO_3$-400 contains 6 nm nickel together with residual $LaNiO_3$, which indicates incomplete precursor transformation. $LaNiO_3$-

500 and $LaNiO_3$-600 contain 8 nm nickel and h-La_2O_3, indicating a more complete generation of the nickel–lanthana architecture. The impregnated material contains larger 11 nm nickel domains and larger lanthanum oxide domains. The spent perovskite-derived material contains h-$La_2O_2CO_3$ together with h-La_2O_3, showing that the active material evolves toward an oxycarbonate-containing lanthanum environment rather than remaining a simple oxide. This phase evolution is consistent with a dynamic lanthanum reservoir and is not captured by nickel size alone.

Table 3. Lanthanum surface-state markers used for oxygenate-gate assignment.

Catalyst state	$\Delta_{La\,3d}$ (eV)	CO_3^{2-}/La ratio	Gate assignment
$LaNiO_3$-derived reaction surface	3.6	0.1	open hydroxide/oxycarbonate gate
Ni/La_2O_3 reaction surface	3.4	1.6	carbonate-blocked gate

Table 3 supplies the surface-chemical evidence needed to interpret the lanthanum phase. The difference between a carbonate-to-lanthanum ratio of 0.1 and a ratio of 1.6 is not a minor spectral adjustment; it changes the likely role of carbon on the lanthanum surface. The low ratio for the $LaNiO_3$-derived reaction surface indicates that lanthanum-bound carbon species remain sparse enough to participate in exchangeable hydroxide/oxycarbonate chemistry. The high ratio for impregnated Ni/La_2O_3 indicates a carbonate-rich surface in which carbon species may become spatially and stoichiometrically dominant. The gate assignment therefore converts XPS-derived surface information into a catalyst-design statement: reactive CO_2 capture is favourable only when carbonate formation does not isolate the carbon reservoir from metallic nickel.

4 Results and discussion

4.1 Thermal activation gain and light-off behaviour

On the basis of the reference catalyst (impregnated Ni/La_2O_3), the calculated thermal activation gain is 56 °C, 81 °C, and 96 °C for $LaNiO_3$-400, $LaNiO_3$-500, and $LaNiO_3$-600, respectively, corresponding to light-off improvement by 14.7 %, 21.3 %, and 25.2 %. From the monotonically decreasing trend of T_{50}, one can conclude that the most favourable state in terms of methanation ability is not reached at 400 °C, which is manifested as the residual perovskite phase in $LaNiO_3$-400. In this case, some fraction of nickel in the sample is still inaccessible due to lack of proper transformation of the $LaNiO_3$ structure.

Table 4. Derived catalytic descriptors obtained from the carbon-state-gated interface normalisation method.

Catalyst	ΔT_{50} (°C)	L_i (%)	$E_{app,ref}/E_{app,i}$	N_i (°C nm^{-1})
$LaNiO_3$-400	56	14.7	0.94	8.77
$LaNiO_3$-500	81	21.3	0.97	9.81
$LaNiO_3$-600	96	25.2	1.07	12.83
Ni/La_2O_3	0	0.0	1.00	0.00

The data in Table 4 allow us to assign a ranking to the catalysts based on performance. First, one sees from the first two columns that all perovskite-derived materials improve the light-off temperature compared with the impregnated material, with an increasingly strong effect at higher temperatures. The second descriptor in the table is the ratio of the apparent activation energy of the target reactions. It is less than unity for $LaNiO_3$-400 and $LaNiO_3$-500, which indicates that the reaction is faster than on the comparator at these temperatures due to high activation energy. For $LaNiO_3$-600, however, the ratio is *larger* than unity, meaning that the difference is caused by both improved light-off and lowered kinetic barrier. Therefore, the third column clearly shows the highest N_i for this material. Thus, it is clear from the descriptor table that the optimal material is not simply a cool-light-off version of the impregnated comparator.

The light-off and activation energy trends are plotted in Figure 2 where the upper plot shows that the difference in T_{50} between perovskite-derived materials and the impregnated comparator increases dramatically from $LaNiO_3$-400 to $LaNiO_3$-500 to $LaNiO_3$-600. The lower plot of apparent activation energy makes it clear that, unlike $LaNiO_3$-400 and $LaNiO_3$-500, $LaNiO_3$-600 also reduces this parameter.

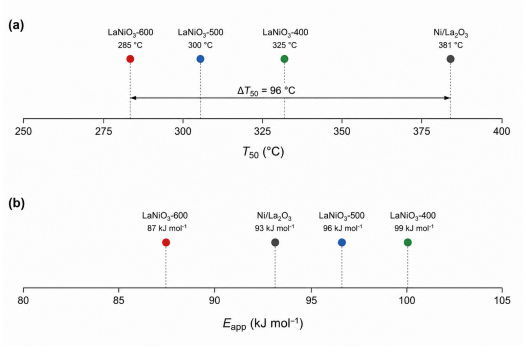

Figure 2. Comparison of light-off and apparent-activation energy for the perovskite-derived catalyst series and impregnated Ni/La_2O_3. The figure shows that $LaNiO_3$-600 features the highest light-off gain and the lowest apparent activation energy.

The analysis above highlights a role of the activation protocol used to synthesise the catalyst. The transition from $LaNiO_3$-400 to $LaNiO_3$-600 does not simply mean a higher temperature in the activation step. Indeed, in the case of $LaNiO_3$-400, the presence of the perovskite phase prevents the full transformation of the nickel oxide structure leading to a relatively small gain in light-off temperature. Activation at 500 °C already shows significant progress in terms of the formation of metallic nickel, while the apparent activation energy does not reach the lowest value. Only the activation at 600 °C enables sufficient transformation that results in an optimal nickel oxide composition, h-La_2O_3, and a suitable surface-carbon state.

4.2 Size-normalised activity gain

The next test assesses the significance of the observed light-off gain after correcting it by taking into account nickel particle size. The size-only ranking would give the first position to $LaNiO_3$-400 since it has the smallest nickel size, i.e., 6 nm. However, the calculated descriptors contradict this assumption. The size-normalised ranking is

$$LaNiO_3 - 600 > LaNiO_3 - 500 > LaNiO_3 - 400 > Ni/La_2O_3.$$

Thus, nickel size is definitely not the sole factor influencing the methanation rate. Even though $LaNiO_3$-600 features 8 nm nickel size, it shows the highest light-off gain and the lowest apparent activation energy. This material exhibits the highest $N_i = 12.83\,^{\circ}\mathrm{C\,nm^{-1}}$, i.e., each additional nanometre of nickel crystallites leads to an increasingly strong low-temperature advantage.

The smaller value of $LaNiO_3$-400, $N_i = 8.77\,^{\circ}\mathrm{C\,nm^{-1}}$, although much lower than for the most favourable material, provides scientific evidence of improved catalytic interface. Indeed, the residual perovskite phase and somewhat high activation energy indicate that the material has not reached a sufficiently transformed state yet. However, the light-off improvement and the lower value of N_i for $LaNiO_3$-500 suggest the progress in the development of the desirable material. Still, the activation energy in the latter case is significantly higher than for the best sample. Apparently, the decisive improvement in catalyst performance and kinetics takes place with activation at 600 °C.

(a) Light-off gain vs. nickel size. **(b)** Size-normalised descriptor ranking.

Figure 3. The size-normalised assessment of methanation reactivity and kinetics. The figure illustrates that the best state among the studied samples is not the sample with the smallest nickel size.

Figure 3 demonstrates a direct graphical illustration of the previous arguments. First, one can see that even though nickel crystallites in $LaNiO_3$-400 are smaller than in the other samples, this material shows the lowest size-normalised activity gain. This result is summarised in panel (b), in which the ranking of size-normalised descriptors is shown. As

can be seen, nickel size alone is not informative of a material's ability to perform a particular chemical reaction, and the material design should include a combination of various factors such as particle size, accessibility of metallic phase, and kinetic energy requirements.

4.3 Lanthanum oxygenate gate and surface-state selectivity

The decisive chemical aspect that distinguishes perovskite-derived materials from the impregnated comparator is the oxygenate gate. The perovskite-derived reaction surface is identified as an open gate since the splitting of the La 3d signal is 3.6 eV and the carbonate-to-lanthanum surface ratio is approximately 0.1. This surface configuration corresponds to a lanthanum oxide phase compatible with hydroxide formation and evolution towards oxycarbonate formation. The spent-phase analysis supports this interpretation with the presence of h-$La_2O_2CO_3$ together with h-La_2O_3. Thus, the evolution of active lanthanum phase towards oxycarbonate formation is not simply depositing an inert species, but the continuation of the formation process of the interface required for methanation.

Conversely, the impregnated Ni/La_2O_3 reaction surface features different characteristics: the splitting of the La 3d signal is close to 3.4 eV and the carbonate-to-lanthanum ratio is about 1.6. Thus, there is a high probability that this sample will feature an inactive carbon species on its lanthanum surface. It is indeed expected, since the presence of carbonates on the lanthanum surface can prevent the hydrogen from reaching nickel–lanthana boundary sites.

A distinction between open and blocked surfaces explains the apparent contradictions in previously reported studies on lanthana-based methanation. Specifically, research on carbonate modified lanthanum surfaces revealed that metal–carbonate interactions contribute positively to the selectivity of methanation process [5, 6]. In turn, recent reports demonstrated the beneficial role of hydroxides and oxycarbonates on the surface of $LaNiO_3$-derived methanation catalysts and the negative influence of carbonate species [7]. The current oxygenate gate explanation unifies these results as a difference between favourable active interfaces (hydroxide and oxycarbonate-containing surface of lanthana oxide) and inactive interfaces (stoichiometric carbonate).

(a) Gate map. **(b)** Comparison of surface states.

Figure 4. Surface-characterisation parameters used for distinguishing between open hydroxide/oxycarbonate-compatible and blocked carbonate-containing interfaces. Perovskite-derived reaction surface is characterized by a 3.6 eV La 3d splitting and low carbonate abundance, while impregnated Ni/La_2O_3 surface is characterized by a 3.4 eV splitting and high carbonate abundance.

To visualise the difference between the perovskite-derived and the impregnated catalysts in terms of surface states, let us represent them on the surface-state plane in Figure 4. First, panel (a) shows that the two materials correspond to completely different regions in the splitting vs. carbonate ratio space. Second, one can see from panel (b) that the impregnated sample is characterised by a significantly higher amount of carbonates. As can be seen from the discussion above, the presence of carbonates on lanthanum surface does not guarantee efficient methanation process.

4.4 Integrated mechanism of the favourable interface

The calculated descriptors help to formulate a three-step model of methanation for the favourable $LaNiO_3$-600 state. First, nickel is separated from the lattice and forms metallic nickel islands. The approximate 8 nm size of nickel crystallites enables creation of active nickel–lanthana boundary positions, but keeps the size smaller than that in impregnated Ni/La_2O_3 where the domains reach 11 nm. Moreover, activation at 600 °C enables complete removal of residual perovskite structure, thus making the nickel–lanthana interface clean.

Second, CO_2 interacts with lanthanum oxygen to create carbon-oxygen-containing surface species. These species do not form stoichiometric carbonate, but lead to the formation of lanthanum oxide with properties allowing hydroxide and oxycarbonate formation. Thus, in the most efficient material, hydrogen can reach the interface and undergo sequential hydrogenation on nickel and carbon–oxygen sites to produce methane. The relatively low apparent activation energy of the perovskite-derived material supports this interpretation, showing that the limiting steps in the process have a low energy.

For the impregnated Ni/La_2O_3 sample, the functional ingredients of methanation are present, but the arrangement is suboptimal. The nickel particles in this sample are slightly larger and the lanthanum surface is enriched in carbonates. A ratio of 1:6 means high carbon abundance on the catalyst surface, but in view of high enrichment, the surface may prevent efficient hydrogen transfer to carbon–oxygen positions. The key point of the discussed material, thus, is the importance of coupling between the active phases: both a carbon surface species and a metal surface must be present. Without such coordination, the material will have low methanation performance, despite the presence of nickel and lanthanum.

In discussing the spent-phase evolution, the same interpretation is needed as for the previous point. Namely, a lot of research focuses on carbonate formation and treats it as a detrimental deactivation phenomenon. However, it should be clarified that, in the perovskite-derived sample, carbonate formation may be viewed as evolution of the interface towards increased reactivity. In the comparator, it is indeed a sign of an inactive lanthanum surface, and it is important that the same term, "carbonate", includes two different processes depending on the specific reaction conditions and lanthanum surface phase identity.

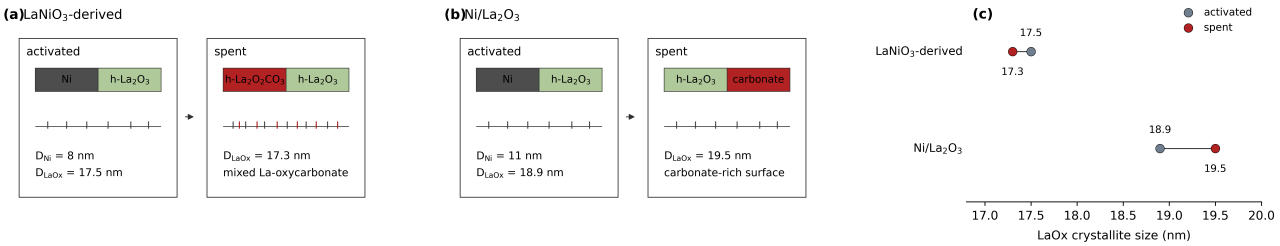

(a) $LaNiO_3$-derived sequence. **(b)** Impregnated sequence. **(c)** D_{LaOx} comparison.

Figure 5. Phase-evolution comparison for perovskite-derived and impregnated nickel–lanthana catalysts. The figure links activated-state phase identity, spent-state lanthanum chemistry, and lanthanum oxide domain size to the open or blocked surface-carbon state.

Figure 6 connects the gate assignment to bulk and near-surface phase evolution. The perovskite-derived material moves from activated h-La_2O_3 to a spent state containing h-$La_2O_2CO_3$, whereas the impregnated comparator retains an oxide-dominated crystalline description while carrying a carbonate-rich surface. The small change in lanthanum oxide domain size for the perovskite-derived route suggests controlled chemical reconstruction rather than severe oxide coarsening. The figure therefore supports the interpretation that the favourable catalyst is formed by a managed transformation sequence, not by a simple increase in total crystallinity.

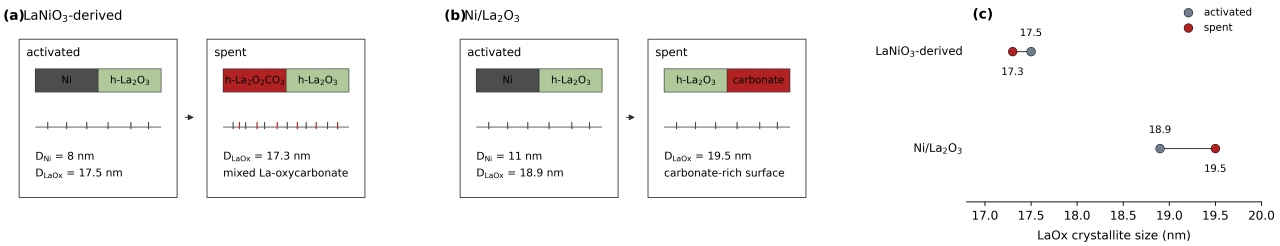

(a) $LaNiO_3$-derived sequence. **(b)** Impregnated sequence. **(c)** D_{LaOx} comparison.

Figure 6. Phase-evolution comparison for perovskite-derived and impregnated nickel–lanthana catalysts. The figure links activated-state phase identity, spent-state lanthanum chemistry, and lanthanum oxide domain size to the open or blocked surface-carbon state.

Figure 6 connects the gate assignment to bulk and near-surface phase evolution. The perovskite-derived material moves from activated h-La_2O_3 to a spent state containing h-$La_2O_2CO_3$, whereas the impregnated comparator retains an oxide-dominated crystalline description while carrying a carbonate-rich surface. The small change in lanthanum oxide domain size for the perovskite-derived route suggests controlled chemical reconstruction rather than severe oxide coarsening. The figure therefore supports the interpretation that the favourable catalyst is formed by a managed transformation sequence, not by a simple increase in total crystallinity.

Figure 7 provides the mechanistic interpretation of the full descriptor set. In the open case, the nickel particle and lanthanum oxygenate region act as a coupled reaction zone. Hydrogen activation and carbon–oxygen activation remain spatially connected, making methane formation more accessible at lower temperature. In the blocked case, carbonate enrichment partially decouples the two functions. The figure therefore explains why $LaNiO_3$-600 outperforms impregnated Ni/La_2O_3 even though both materials contain nickel and lanthanum oxide.

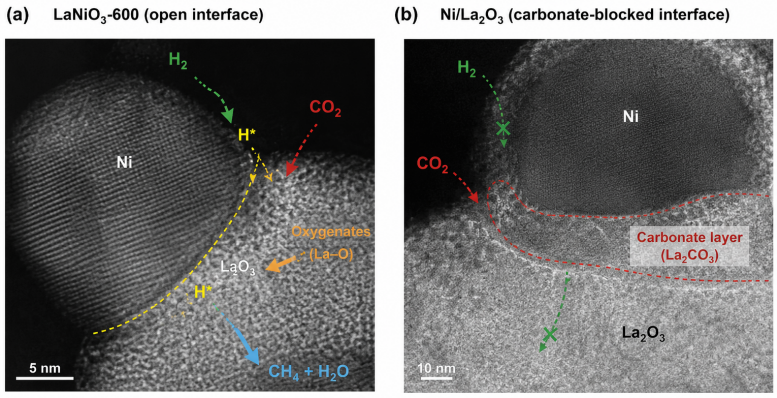

Figure 7. Mechanistic contrast between the open $LaNiO_3$-derived interface and carbonate-blocked impregnated Ni/La_2O_3. The open interface preserves contact among metallic nickel, hydrogen-derived species, and labile lanthanum oxygenates, whereas the blocked interface contains a carbonate-rich layer that restricts access to the nickel–lanthana boundary.

4.5 Stability and materials-design implications

The structural descriptors suggest that the perovskite-derived interface should be more resistant to deactivation than a conventionally impregnated analogue. Exsolved nickel particles are expected to be more strongly anchored than deposited particles, reducing migration and coalescence during thermal operation. This anchoring effect is widely recognised in exsolution chemistry and is one of the main reasons perovskite-derived catalysts are attractive for energy-conversion applications [10–12]. The present analysis adds a further requirement: anchored nickel must remain adjacent to a lanthanum phase whose carbon state is open. Stability is therefore not only a question of resisting sintering; it is also a question of preventing carbonate chemistry from isolating the active boundary.

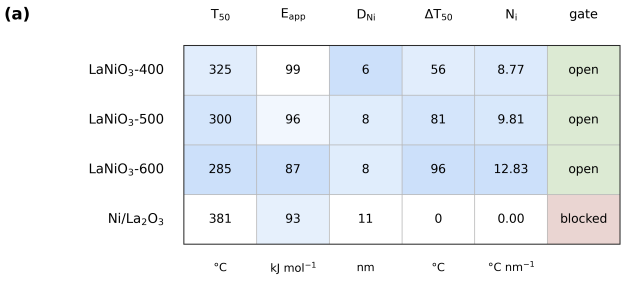

(a)

	T_{50}	E_{app}	D_{Ni}	ΔT_{50}	N_i	gate
$LaNiO_3$-400	325	99	6	56	8.77	open
$LaNiO_3$-500	300	96	8	81	9.81	open
$LaNiO_3$-600	285	87	8	96	12.83	open
Ni/La_2O_3	381	93	11	0	0.00	blocked
	°C	kJ mol^{-1}	nm	°C	°C nm^{-1}	

(a) Integrated descriptor matrix.

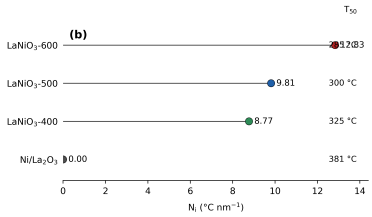

(b) Descriptor ranking.

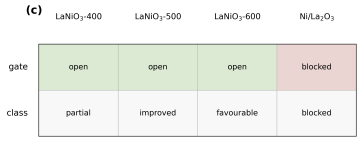

(c) Gate-class strip.

Figure 8. Integrated carbon-state-gated descriptor summary. The matrix, ranking plot, and gate-class strip show that $LaNiO_3$-600 is the only state combining the lowest T_{50}, lowest apparent activation energy, highest N_i, and open oxygenate gate.

Figure 8 condenses the numerical and chemical evidence into a single decision sequence. The matrix shows that LaNiO3-600 satisfies every favourable condition, whereas LaNiO3-400 and LaNiO3-500 satisfy only part of the sequence. The impregnated comparator is limited most strongly by the blocked gate and the absence of a light-off gain. The figure is therefore not only a summary chart; it is the operational answer to the ranking problem. It identifies the catalyst state that simultaneously meets the performance, kinetic, structural, and surface-chemical criteria.

For catalyst design, the results imply that activation should be selected to generate a chemically useful interface rather than to maximise a single measured quantity. Activation at 400 °C gives small nickel particles but incomplete phase

transformation. Activation at 500 °C improves the light-off response but does not reduce the apparent barrier below that of the comparator. Activation at 600 °C gives the best combined response because it balances nickel exsolution, lanthanum oxide formation, and open oxygenate chemistry. This design logic can be transferred to other exsolved catalyst systems only when comparable surface-state markers are available; without them, the method would risk confusing high CO_2 uptake with productive interfacial turnover.

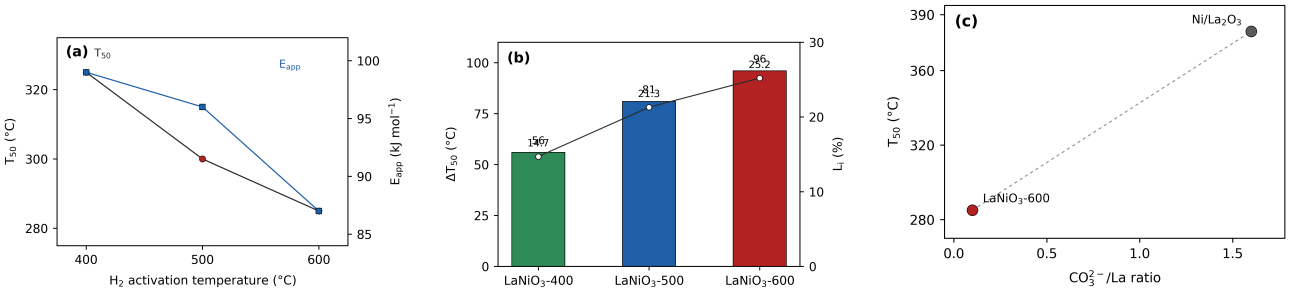

(a) Activation-temperature trend. **(b)** Light-off gain. **(c)** Carbonate ratio and T_{50}.

Figure 9. Materials-design implications of the carbon-state-gated descriptor. The figure links activation temperature, light-off gain, and carbonate-to-lanthanum surface ratio to show why the best low-temperature response appears when nickel exsolution is paired with an open lanthanum oxygenate state.

The result obtained in this paper is illustrated through a design-oriented scheme in Figure 9. While (a) displays the dependence of the T_{50} and E_{app} on perovskite-derived activation temperature, (b) shows the light-off improvement achieved in terms of absolute and relative gains. (c) illustrates the link between T_{50} and carbonate-to-lanthanum ratio, which is a measure of the opening status of the surface oxygenates. Figure 9 thus translates the paper's mechanistic conclusion into a selection guideline for optimal catalysts: the preferred state is not only the most reduced and/or most fine-dispersed material, but also the state where nickel and lanthanum oxygenates are accessible to each other.

This paper also offers a reporting strategy for the results from tests performed on nickel–lanthana methanation materials. In addition to conversions and selectivities, the descriptor analysis requires at least four parameters: nickel domain size, apparent activation energy, lanthanum phase identity post-activation/reaction, and a measure of the surface-state marker that distinguishes between hydroxide/oxycarbonate chemistry and carbonate buildup. Without such information, a seemingly good material in terms of light-off performance might have a surface state that is unlikely to remain active throughout the process. Alternatively, a relatively poorly dispersed material might prove highly effective provided that the surface state ensures easy accessibility to a dynamically open metal-oxide boundary.

From the point of view of materials technology, the present paper adds perovskite-derived nickel–lanthana catalysts to the family of adaptive functional materials. As adaptive functional materials, their significance lies in their ability to form a catalytically active metal-oxide boundary, which emerges only during activation and operation. This makes the carbon-state-gated approach a direct means to connect synthesis, activation, and catalysis in relation to a specific carbon-utilisation process.

5 Conclusions

In summary, the question addressed in this paper was: given the light-off behaviour, apparent activation energy, nickel crystallite size, lanthanum phase evolution, and surface-carbon chemistry, what is the most effective interface for catalysing low-temperature CO_2 methanation? This paper answered that the optimal state is $LaNiO_3$-600, which shows 50% CO_2 conversion already at 285 °C, which is 96 °C below impregnated Ni/La_2O_3. $LaNiO_3$-600 also produces a 25.2 % light-off improvement, which is larger than those of other catalyst states; has the lowest apparent activation energy (87 kJ mol^{-1}); and yields the largest size-normalised activity gain (12.83 °C nm^{-1}).

The present paper demonstrates that nickel domain size alone cannot explain the ranking. $LaNiO_3$-400 has the smallest particles, approximately 6 nm diameter, but it is the worst-performing state in terms of relative size-normalised gain. Although $LaNiO_3$-600 has slightly bigger particles (8 nm diameter), it surpasses the smaller particles owing to the coupling of nickel particles to a reactive lanthanum phase. Overall, the present paper answers the design question stated at the outset, demonstrating that the best nickel–lanthana methanation catalyst is that with easily accessible nickel domains and chemically reactive lanthanum oxygenates.

The surface-state analysis is key for distinguishing between exsolved perovskite-derived materials and their impregnated counterparts. Exsolved perovskite-derived reaction surface features a La 3d splitting around 3.6 eV and a carbonate-to-lanthanum ratio of approximately 0.1, corresponding to an open hydroxide/oxycarbonate gate. The impregnated Ni/La_2O_3 reaction surface features a splitting near 3.4 eV and a ratio of ≈ 1.6, corresponding to a carbonate-blocked gate.

An open gate is thus produced if metallic nickel particles retain easy contact to a labile lanthanum oxide environment. A less effective gate is produced if carbonate enrichment isolates the carbon reservoir from the hydrogenation region.

Overall, the general implication of this study is that exsolved perovskite-derived catalysts need to be assessed as adaptive materials, rather than static composites of metal particles and oxide environment. In the case of nickel–lanthana methanation catalysts, a proper description of catalysts needs to include T_{50}, E_{app}, nickel domain size, lanthanum phase, and a carbon-state marker. The carbon-state-gated normalisation technique can then be used to obtain the information necessary to determine whether the material has an open surface state. With respect to the present series, $LaNiO_3$-600 emerged as the preferred state and demonstrated how to design catalysts for low-temperature methane formation.

Acknowledgements

No external financial support was received for this study.

Numerical-value availability

All numerical values used for the descriptor calculations are contained in Tables 1–3. The calculated quantities are reported in Table 4.

Conflict of interest

The authors declares no conflict of interest.

References

[1] S. Rönsch, J. Schneider, S. Matthischke, M. Schlüter, M. Götz, J. Lefebvre, P. Prabhakaran and S. Bajohr, Review on methanation: From fundamentals to current projects, *Fuel*, 2016, 166, 276–296.

[2] X. Su, J. Xu, B. Liang, H. Duan, B. Hou and Y. Huang, Catalytic carbon dioxide hydrogenation to methane: A review of recent studies, *Journal of Energy Chemistry*, 2016, 25, 553–565.

[3] C. Vogt, M. Monai, G. J. Kramer and B. M. Weckhuysen, The renaissance of the Sabatier reaction and its applications on Earth and in space, *Nature Catalysis*, 2019, 2, 188–197.

[4] W. Wang, S. Wang, X. Ma and J. Gong, Recent advances in catalytic hydrogenation of carbon dioxide, *Chemical Society Reviews*, 2011, 40, 3703–3727.

[5] Y. Dai, M. Xu, Q. Wang, R. Huang, Y. Jin, B. Bian, C. Tumurbaatar, B. Ishtsog, T. Bold and Y. Yang, Enhanced activity and stability of $Ni/La_2O_2CO_3$ catalyst for CO_2 methanation by metal–carbonate interaction, *Applied Catalysis B: Environmental*, 2020, 277, 119271.

[6] C. Zhong, Y. Yang, J. Chen, B. Feng, H. Wang and Y. Yao, Nickel nanoparticles supported on lanthanum oxycarbonate with interfacial oxygen vacancies as catalysts for CO_2 hydrogenation to methane, *ACS Applied Nano Materials*, 2024, 7, 14057–14068.

[7] M. Barreau, D. Salusso, J. Zhang, M. Haevecker, D. Teschner, A. Efimenko, F. Bournel, J.-J. Gallet, E. Borfecchia, K. Sobczak, C. Petit and S. Zafeiratos, Uncovering the critical function of lanthanum in CH_4 production from CO_2 using exsolved $LaNiO_3$ perovskite catalysts, *Journal of Materials Chemistry A*, 2024, 12, 7605–7621.

[8] A. Olafsen Sjastad, A.-K. Larsson, H. Fjellvag and B. C. Hauback, On the crystal structure of $Ln_2O_2CO_3$ II (Ln = La and Nd), *Journal of Solid State Chemistry*, 2001, 158, 14–24.

[9] E. Çiftçi, S. Leising, C. Wickleder and H. Huppertz, Crystal structure and spectral characterization of $La_2(CO_3)_3 \cdot 5\,H_2O$, *Zeitschrift für anorganische und allgemeine Chemie*, 2022, 648, e202200218.

[10] D. Neagu, T.-S. Oh, D. N. Miller, H. Ménard, S. M. Bukhari, S. R. Gamble, R. J. Gorte, J. M. Vohs and J. T. S. Irvine, Nano-socketed nickel particles with enhanced coking resistance grown in situ by redox exsolution, *Nature Communications*, 2015, 6, 8120.

[11] K. Kousi, C. Tang, I. S. Metcalfe and D. Neagu, Emergence and future of exsolved materials, *Small*, 2021, 17, 2006479.

[12] J. Wu, R. Ye, D. J. Xu, L. Wan, T. R. Reina, H. Sun, Y. Ni, Z. F. Zhou and X. Deng, Perovskite exsolution catalysts for energy conversion, *Frontiers in Chemistry*, 2022, 10, 961355.